NASA TECHNICAL NOTE

NASA TN D-5747

NASA TN D-5747

COMPUTER-MADE MOTION PICTURES AND TIME HISTORY PLOTS OF ION — POLAR-MOLECULE COLLISIONS

by John V. Dugan, Jr., R. Bruce Canright, Jr., and Raymond W. Palmer

Lewis Research Center
Cleveland, Ohio 44135

NATIONAL AERONAUTICS AND SPACE ADMINISTRATION • WASHINGTON, D. C. • JUNE 1970

1. Report No. NASA TN D-5747	2. Government Accession No.	3. Recipient's Catalog No.
4. Title and Subtitle COMPUTER-MADE MOTION PICTURES AND TIME HISTORY PLOTS OF ION - POLAR-MOLECULE COLLISIONS		5. Report Date June 1970 6. Performing Organization Code
7. Author(s) John V. Dugan, Jr., R. Bruce Canright, Jr., and Raymond W. Palmer		8. Performing Organization Report No. E-5250
9. Performing Organization Name and Address Lewis Research Center National Aeronautics and Space Administration Cleveland, Ohio 44135		10. Work Unit No. 129-02 11. Contract or Grant No. 13. Type of Report and Period Covered
12. Sponsoring Agency Name and Address National Aeronautics and Space Administration Washington, D.C. 20546		Technical Note 14. Sponsoring Agency Code

15. Supplementary Notes

Film Supplement C-269 available on request.

16. Abstract

Motion pictures and time history plots of ion-dipole collisions involving the polar molecules CO, HCl, and CH_3CN have been made using a computer-plotter. The three polar molecules studied cover a range of dipole moments and moments of inertia of interest in ion-molecule collisions. The results of numerical integration are stored on magnetic tape and processed by the IBM 360/67 using calls to subroutines of the CDC DD280 plotter system. These plot results on 35-millimeter film are made into black-on-white prints, whereas the motion pictures are converted to 16-millimeter white-on-black. The collision motion pictures provide instantaneous correlation of translational (ion) and rotational (dipole) motion during interaction. The motion-picture results and time history plots complement each other in providing qualitative and quantitative results of collision behavior. All three polar rotators are hindered by the incident ion; the nature and chemical aspects of this hindered rotation are discussed.

17. Key Words (Suggested by Author(s))	18. Distribution Statement
Ion-molecule Polar-molecule Computer motion pictures	Unclassified - unlimited

19. Security Classif. (of this report)	20. Security Classif. (of this page)	21. No. of Pages	22. Price*
Unclassified	Unclassified	36	$3.00

*For sale by the Clearinghouse for Federal Scientific and Technical Information Springfield, Virginia 22151

COMPUTER-MADE MOTION PICTURES AND TIME HISTORY PLOTS OF ION - POLAR-MOLECULE COLLISIONS*

by John V. Dugan, Jr.; R. Bruce Canright, Jr., and Raymond W. Palmer

Lewis Research Center

SUMMARY

Motion pictures and time history plots of ion-dipole collisions involving the polar molecules carbon monoxide (CO), hydrochloric acid (HCl), and methyl cyanide (CH_3CN) have been made using a computer-plotter. The three polar molecules studied cover a range of dipole moments and moments of inertia of interest in ion-molecule collisions. The results of numerical integration are stored on magnetic tape and processed by the IBM 360/67 using calls to subroutines of the CDC DD280 plotter system. These plot results on 35-millimeter film are made into black-on-white prints, whereas the motion pictures are converted to 16-millimeter white-on-black. The collision motion pictures provide instantaneous correlation of translational (ion) and rotational (dipole) motion during interaction. The motion-picture results and time history plots complement each other in providing qualitative and quantitative results of collision behavior. All three polar rotators are hindered by the incident ion; the nature and chemical aspects of this hindered rotation are discussed.

INTRODUCTION

Numerical calculations have been reported for capture cross sections in collisions between ions and polar molecules (refs. 1 and 2). These capture cross sections, which are upper limits to reaction cross sections, are in good agreement with experiment (ref. 3). Capture is defined as the approach of ion and molecule within an initially specified ion-molecule separation. These computer studies have been extended to plotting time histories of relative velocity, polar-molecule rotational energy, and ion-dipole orientation angle against ion-molecule separation (refs. 4 to 6). Time histories of the

*Presented at Sixth International Conference on Physics of Electronic and Atomic Collisions, MIT, Cambridge, Mass., July 28 - Aug. 2, 1969.

dipole unit vector and the ion trajectory relative to the dipole have also been plotted to study the nature of the interaction and to calculate collision times.

The ion translational motion has been studied by means of plots of coordinate angles which describe orbital behavior. Spiraling, as conventionally defined (refs. 5 and 6), does not occur in Langevin (pure polarizability) collisions. The cumulative effect of multiple reflections off a repulsive potential can, however, produce a net circuit of the ion around the polar molecule. The presence of the dipole is necessary for multiple-reflection collisions, which generally have much longer collision times than single-reflection collisions (refs. 5 and 6).

Computer-made motion pictures are an excellent means for observing the ion translational and dipole rotational motion instantaneously. The rotational motion of the polar molecule is oscillatory because of the ion - permanent dipole $-\mu e \cos(\gamma/r^2)$ term, where μ is the permanent electric dipole moment, e is the electronic charge, γ is the ion-dipole orientation angle, and r is the ion-molecule separation. The degree to which the rotator can be hindered is of chemical interest (ref. 7) and should be clarified by cinematic studies. This report illustrates the usefulness of studying ion-molecule collisions by means of both motion pictures and still plots.

A motion-picture supplement (C-269) has been prepared and is available on loan. A request card and a description of the film are included at the back of this report.

COLLISION SPECIES

The approximation of a classical ion-dipole plus ion-induced dipole (polarizability) potential has been used with a hard-sphere reflecting barrier to study collisions. A hard-sphere reflection is performed when the radius is equal to the reflection distance r_c; this barrier simulates the ion-molecule repulsion caused by the interacting electronic clouds.

The characteristics of the polar molecule determine the nature of the collisions since the ion is treated merely as a point charge. The ion-molecule interaction potential consists of the ion-dipole and polarizability (ion-induced dipole) $-\alpha e^2/2r^4$ terms, where α is electronic polarizability. In the limit of small dipole moment (carbon monoxide (CO)), the polarizability term dominates the interaction and can cause capture (i.e., the separation becomes less than the reflection distance r_c). This reflection distance is the ion-molecule separation at which the sign of the radial velocity is changed to simulate the short-range electronic repulsion of ion and molecule. However, the dipole does introduce multiple-reflection behavior (refs. 5 and 6). In the limit of large dipole moment (methyl cyanide (CH_3CN)), the strong ion-dipole interaction term determines the trajectory turning points at large separations, in addition to causing multiple reflections. The hydrochloric acid (HCl) molecule has an intermediate value of dipole

moment and a relatively small moment of inertia. The latter characteristic is probably responsible for the low probability of HCl multiple-reflection collisions.

COMPUTER APPROACH

Collision quantities such as ion velocity and dipole rotational energy are plotted using values obtained by numerical integration. The time history plots use the coordinate system where the polar molecule is fixed at the origin. The differential equations of motion are integrated by using the variable-step-length Runge-Kutta scheme of reference 8. Solutions of the equations include the coordinates for motion-picture models of the colliding partners. The initial conditions and calculated values from successful steps (for variables and time derivatives) are stored in a plotting array for both computer-made time history plots and motion pictures. Successful steps are those in which energy is conserved within a certain specified tolerance, usually 1 part in 10^4. After the integration is completed, the plotting subroutines are called. Each plotting array contains $N + 1$ values, where N is the number of successful integration steps (typically, 300 to 1000).

The numerical solutions of the Lagrangian equations of motion are obtained on the IBM 7094 II/7044 or 7094 II/7040 Direct Couple Systems (DCS). The integration histories of all variables (including motion-picture frame coordinates) used in plotting are written onto magnetic tape. The magnetic tape is then processed on an IBM 360/67 running under its time-sharing system. The negative frames for motion pictures or time history plots (black traces on clear background) are made by an on-line Control Data Corporation Model DD280 microfilm recorder which takes photographs of a cathode-ray display tube. The time history photographs are made by connecting the $N + 1$ plot points by N straight lines. The program provides the option of plotting a set of points for every P^{th} step. The microfilm recorder is called by means of a software package developed at Lewis (ref. 8) which provides microfilm plotting subroutines. These subroutines allow for a wide range (type and size) of characters (letters and symbols) for both the motion-picture frames and plot legends.

MOTION-PICTURE MODEL

A typical motion-picture frame is shown in figure 1. The projections of the ion and molecule models are located in the center-of-mass coordinate system where the center of mass is at the origin. Collisions are intrinsically three-dimensional; hence, there is no unique collision plane which can be determined a priori. A collision is followed in an arbitrarily chosen Cartesian plane in which the ion and center of mass are positioned

at the start of a computer run. Each frame shows the locations of the ion, represented by a positive sign surrounded by a ring of dots of varying radius, and of the polar molecule, represented by a dipole similarly ringed. The radii are varied to give the three-dimensional effect that the ion and/or molecule can be above or below the arbitrarily chosen plane. The sum of the two radii is a constant equal to the input reflection distance r_c; r_c values assigned for motion pictures were 2, 2.5, and 3 Å. These values of r_c were chosen by scaling down values of molecular radii obtained from gas viscosity and microwave broadening data (ref. 9). The sum of the ion and molecule radii was chosen to be somewhat less than values given for neutral molecule pairs, even more so for the small diatomic CO. The radius of each varies linearly from $0.75\ r_c$ (10 Å above the approach plane) to $0.25\ r_c$ (10 Å below the approach plane). The ion and molecule are depicted for the time during which this projection in the approach plane is less than 10 Å from the origin. The initial ion-molecule separation is 25 Å; thus the particle models are depicted shortly after the ion begins its approach. In figure 1, the projection of the dipole assumes nearly its full length while rotating almost in the approach plane of the incident ion.

A clock is drawn in the upper right-hand corner of each frame. It consists of a diamond moving about a dot. One complete rotation represents 10^{-13} seconds real time. Since a variable-step-size routine is used, the clock runs at variable speed. The arrow on the dipole in figure 1 does not appear on the actual motion-picture frame; it is used in figure 1 to indicate the instantaneous direction of rotation of the dipole.

FILM PROCESSING

The 35-millimeter motion pictures developed initially in black-on-clear background offer too much glare for comfortable viewing, so the 35-millimeter strips are converted to 16-millimeter white-on-black. The individual time history plots or motion-picture frames for use in research reports are magnified to $8\frac{1}{2}$ by 11 inches, viewed and printed. However, it is difficult to find the proper exposure for obtaining satisfactory white-on-black positive prints from the original negatives. Moreover, these prints reproduce poorly on electrostatic copying machines. Therefore, the 35-millimeter originals are reversed to white-on-black by using the Metro-Kalvar Model 135/16 Microfilm Printer-Processer. High-resolution prints are then made using the reversed film. The most desirable way to study the collision motion pictures is with a variable-speed projector. This yields the best compromise for viewing both rotational and translational motion.

COMPUTER RUNNING TIMES

The execution time for integrating a trajectory varies widely for the polar molecules studied since it is principally a function of their moments of inertia. The collisions were studied for the same initial velocity (5×10^4 cm sec^{-1}) with rotators chosen randomly from a distribution of rotational energies E_R at rotational temperature T_R = 300 K. Collisions involving "hot" HCl rotators ($E_R > kT_R$, where k is the Boltzmann constant) required as many as 35 000 integration steps, and execution times (on the 7094) were as long as 2 to 5 minutes. On the other hand, the average execution time for a representative CO case is approximately 5 to 15 seconds (35 to 40 successful steps per second), and about 5 to 10 motion-picture frames per second are written on magnetic tape. Thus, a representative motion picture of 1200 frames requires about 150 seconds of DCS execution time and runs for 50 seconds of viewing time at 24 frames per second. On the other hand, the time histories which are entire sets of points comprising one 35-millimeter plot take only several seconds of execution time.

In addition to execution time, time is required for making the film (for plots or motion pictures) using the 360/67 - DD280 system. For a 1000 to 2000 frame motion picture, the film requires approximately 10 minutes of actual processing time. In the time-sharing mode, the job might actually require a considerably longer period.

SUMMARY OF TIME HISTORY RESULTS

The coordinate systems and variables used to describe ion-dipole interaction for linear and symmetric-top targets have been extensively discussed (refs. 2 to 6). The probability of multiple reflections, as well as the shape of the ion orbits in the dipole field, has been studied (refs. 4 to 6). Results shown are for rotators chosen from a heat bath at 300 K with incident ions having energy equal to kT at 300 K, where T is the translational temperature of the ion-molecule system. Initial conditions on coordinates and time derivatives are chosen randomly given these energies. The results for collision times and reflection probabilities are included in table I. The fraction of multiple-reflection collisions is highest for CH_3CN (large dipole moment, large principal moment of inertia), approximately 0.5 for impact parameters from 3 to 10 Å. Most CH_3CN collisions were studied for a reflection distance r_c of 2 Å. The fraction of reflections f_R is about the same for CO for impact parameters of 2 and 6 Å and r_c values of 1 or 2 Å. The most probable number of reflections is highest for CH_3CN and lowest for CO. However, the maximum number of reflections observed was greatest for HCl, leading to the longest collision times of nearly 10^{-10} seconds. It appears that these latter collisions satisfy some resonance criterion for HCl captures (ref. 6).

The rotational-translational energy exchange is clear from plots of relative velocity

and rotational energy against ion-molecule separation r. The acceleration-deceleration ion motion and oscillating rotational energy patterns are characteristic of all these targets for multiple-reflection capture collisions (ref. 6). The turning points for the ion-molecule capture complexes are proportional to the dipole moment and vary from 2 to 5 Å for CO to 3 to 22 Å for CH_3CN[6]. The capture cross sections for these targets range from 150 $(Å)^2$ (Langevin) for CO at translational thermal energy (0.026 eV) to 750 $(Å)^2$ for CH_3CN[3] at the same relative energy. The capture cross-section values naturally restrict the region of interest to impact parameters at which multiple reflection is studied. The nature of the ion orbit is easily seen in plots of the coordinate angles θ and φ in the polar-molecule coordinate system shown in figure 2. The plots of time variation of dipole unit vector (located by angles ξ and η) and ion-dipole orientation angle complement the motion pictures for studying hindered rotation.

RESULTS AND DISCUSSION

In the following discussion, the ion approach plane is the X-Y plane, where the ion first starts toward the polar molecule, with the polar molecule at the origin. The time history plots are made in this coordinate system (fig. 2). Transformations are made to the center-of-mass system to make motion-picture frames. The origin of this system is always midway between ion and molecule.

Collisions of Ar^+ with CO

Ar^+ + CO single reflection. - The still plots for a single- (not specular) reflection CO collision are shown in figures 3 to 5. The variation of the ion velocity (fig. 3(a)) is quite similar to that for CO Langevin collisions because the polarizability interaction remains dominant. The ion-induced dipole term is approximately 10 times the maximum ion-dipole term (i.e., $\cos \gamma = 1$). The ion-dipole term is nevertheless large enough to increase the rotational energy from 0.25 to 0.75 kT_R (fig. 3(b)). The dipole rotation does introduce an asymmetry in the trajectory, as shown in the ion orbit plots of figure 4. The reflection takes place below the X-Y plane in the polar-coordinate system (fig. 4(a)).

The CO single-reflection variation of dipole unit vector coordinates is shown in figure 5. The rotator appears relatively free (double traces indicating perturbed rotation) until hindering occurs at several Å. This is shown in the orientation angle plot of figure 5, where the higher frequency trace shows post-reflection behavior. The rod is "heated" and rotates freely in the X-Y plane after reflection, as indicated by the dark trace of rotator projections. This straight-forward interpretation of rotational behavior

is to be contrasted with interpretation of certain multiple-reflection cases. This single-reflection case is the first collision shown in the film supplement.

The CO single-reflection sequence shows only a slight hindering of the polar rotator at 2 to 3 Å (i.e., during reflection) followed by an acceleration of the target. The ion does a partial circuit about the CO molecule, then returns to large separations. The CO dipole completes several rotations before and after the short-range reflection. The film supplement shows that the oscillatory rotational motion is relatively free.

CO multiple reflection. - The time histories for a multiple-reflection CO capture collision are shown in figures 6 to 9. The plots are not retraced to the initial separation $r_0 = 25$ Å because the plot capacity was exceeded. The acceleration-deceleration pattern of the ion velocity (fig. 6(a)) is characteristic of multiple-reflection collisions with just several reflections. The rotational energy variation shown in figure 6(b) suggests not only that the rotator is heated (E_R increased) but also that the ion-dipole orientation is changed since the oscillation frequency is considerably increased. The heating of the rotator is similar to that of the CO single-reflection case and is representative behavior for a capture collision where the initial ion energy exceeds the target rotational energy. Some detail is omitted in the figure 7 plot of ion-dipole orientation angle because only every second point was plotted. The initial unit vector plot of the dipole is nearly in the X-Y plane of figure 2. The rod is actually less hindered during reflection than in the single-reflection collision (see fig. 7 rotator projections and orientation angle γ). The rapid variation in γ is consistent with the post-reflection variation in rotational energy. Capture is mainly the result of the ion translational motion locking "in phase" with the motion of the attractive (negative) end of the rotating dipole.

Figure 8 shows variations of the coordinate angles which are typical of multiple-reflection ion-dipole collisions (ref. 6). The reflections occur below the approach plane (fig. 8(a)). Figure 9 shows the variation of ion projections in the three Cartesian planes; the ion appears to undergo approximately 120° scattering off the dipole because of the cumulative effect of reflections. This multiple-reflection case is the second collision shown in the film supplement.

Advantage of Motion Pictures in Interpretation of Time Histories

Motion pictures of multiple-reflection collisions are particularly valuable, primarily because the time history plots for these cases become extremely cluttered. They allow the observer to determine whether oscillatory plot behavior is (1) relatively free rotation as expected in the CO case, (2) partially hindered rotation (precession), or (3) the limit of "extremely hindered" rotation (i.e., simple harmonic motion confined to the collision plane).

A useful quantity to predict the extent of this behavior at any ion-molecule separa-

tion is the hindering distance r_h where the field tends to line up the dipole (defined by $r_h = \sqrt{\mu e/E_R}$). For CO, the r_h value is approximately $\sqrt{3}$ times the reflection distance (~2 Å) for $E_R = kT$. The CO rotational energy increases significantly since $\mu e/r_c^2 \approx 3kT_R$. The dipole rotational frequency is sufficiently great that the rotator assumes its attractive phase several times during ion transit. The frequency of rotational energy change depends upon dipole moment, ion-dipole orientation, and initial rotational energy.

In the CO multiple-reflection case shown in figures 6 to 9, the dipole rotational energy is increased at the expense of translational energy of the ion. From figure 6(b) (upper trace) it appears that a much more rapid fluctuation in rotational energy occurs after reflection than before. However, it must be remembered that the figure shows variation with ion-molecule separation, not with time. Moreover, the simultaneous variations in rotational rate and orientation angle are not easily observed from the figures. The film supplement permits a much more direct grasp of these variations. From the film, it can readily be deduced that the rotational energy does in fact fluctuate nearly twice as fast after reflection.

Collisions of NO_2^+ with HCl

NO_2^+ + HCl single reflection. - Figures 10 to 12 illustrate a representative collision. The maximum ion velocity for this collision is larger than for the Ar^+ + CO single-reflection collision previously illustrated. But the ratio of maximum to initial velocity is not simply proportional to the square root of the ratio of dipole moments (see fig. 10(a)). The interaction energy $-\mu e \cos \gamma/r^2$ is proportional to the dipole moment, but the ratio of this energy to the initial ion energy is the more relevant parameter. The initial conditions determine the average interaction energy through the cosine of the ion-dipole orientation angle, and in this HCl collision the plane of rotation is initially normal to the plane of the ion's approach. This relatively weak initial interaction ensures little hindering at large ion-molecule separations. The variation in rotational energy of figure 10(b) is regularly periodic, with increasing amplitude before reflection and decreasing amplitude afterwards. The frequency of the rotation is almost unchanged. The rotator is relatively cold, with energy $E_R \approx 0.5\ kT_R$ both before and after reflection. This rotator has a higher rotational frequency than the CO targets because of the small HCl moment of inertia.

The rotator projection plots of figure 11 are somewhat detailed, but it is clear upon careful examination that the plane of the rotator is changed by the interaction. The plot of orientation angle in figure 11 indicates that hindering begins at large separations. The polar angle plot of figure 12 shows that reflection takes place below the approach

plane. This single-reflection case is the third collision shown in the film supplement.

The HCl sequence shows that the rotator varies its rotation plane throughout interaction and is drastically hindered before and after reflection. This confirms the conclusions drawn from the plot of variation in orientation angle.

The fourth collision shown in the film supplement is another single-reflection NO_2^+ + HCl collision in which the rotator is hindered early and barely completes a rotation before reflection.

HCl multiple reflection. - The HCl multiple-reflection case of figures 13 to 16 is an example of a trajectory which required extended running time because of the relatively high-frequency rotational motion. The case required 32 000 integration steps, so only every fifth point was stored for plotting. Of these 6400 points, only 2500 are shown (plot capacity). The changes in velocity and rotational energy in figure 13 are so rapid that the variations form an almost solid area where details of behavior are indistinguishable at small separations.

The rotator projections of figure 14 consist of heavy-lined structure ("balls of yarn") obscuring regions of initial and final conditions. In contrast, the translational motion is relatively simple in the collision plane, as can be seen from the regular pattern of 10 reflections shown in the ion polar angle plot of figure 15. (The ion makes more than a complete circuit of the polar molecule, as seen from the ion projection plots of figure 16.) This multiple-reflection case is the fifth collision shown in the film supplement.

The film supplement shows several complete but perturbed rotations before the strong ion-dipole interaction hinders the rod. It also shows that the oscillation in rotational energy at small separations corresponds to relatively free rotation followed by precession. The likelihood of hindering HCl at intermediate separation is generally greater than for CO since the hindering distance for a rotational energy $E_R = kT_R$ is $r_h = 10$ Å. However, this rotator is quite hot ($E_R = 2.0\ kT_R$), so it is not a representative case.

There are chemical implications to this hindered behavior for ion-molecule reactions; this will be discussed after the CH_3CN results.

Collisions of CH_3CN^+ with CH_3CN

In the film supplement, collisions 6 to 9 comprise a study of the sensitivity of multiple-reflection behavior to the reflection distance r_c. Collisions 6 and 7 involve CH_3CN targets with an r_c value of 3 Å; collision 6 is a single-reflection collision, whereas collision 7 is a four-reflection collision. Collisions 8 and 9 have initial conditions identical to those of collisions 6 and 7, but were studied with a reflection distance of 4 Å. The trajectory of the particles in collision 8 is about identical to the single-

reflection case of collision 6. Collision 9 shows only two reflections to be contrasted with the four reflections observed in collision 7. This is a general result (i.e., an increase in reflection distance decreases the probability of multiple reflections (ref. 6)). Time history plots for these four collisions have been omitted for the sake of brevity.

CH_3CN single reflection. - The peak relative velocity for the CH_3CN - parent ion collision in figure 17(a) corresponds to a translational energy 150 times the initial value. The polar rotator initially has nearly kT_R of energy (fig. 17(b)), but the hindering is so great the rotator energy actually goes to zero at separations as large as 25 Å. The CH_3CN dipole moment (3.92 Debye units) causes a maximum potential interaction $\mu e/r_c^2 \approx 3$ eV = 125 kT_R at the reflection distance for T_R = 300 K.

The extreme hindering of the dipole can be seen from the rotator projection plots of figure 18. The large moment of inertia for CH_3CN is responsible for the very simple trace. The simple variation in orientation angle provides a clear history of the hindered rotation.

This single-reflection collision (collision 7) is a good example to use in discussing the criterion for reflection. The dipole precesses in its attractive phase until reflection occurs. This dipole motion leads to a high radial velocity $\dot{r}$ during approach. When reflection occurs (accomplished by changing the sign of $\dot{r}$), the ion receives a large component of velocity away from the dipole. If the dipole does not change orientation rapidly enough to introduce a reflecting barrier, the ion will escape. For multiple reflections to occur, it is more favorable if the ion retains a significant tangential component of velocity.

CH_3CN multiple reflections. - The variations in velocity and rotational energy of figure 19 indicate strong acceleration-deceleration behavior caused by the ion-dipole interaction. The repulsive phase of dipole orientation is strong enough to actually drive the ion away momentarily before reflection is accomplished. This repulsion occurs at separations of 5 to 10 Å. The orbital behavior shown in figure 20 indicates that the trajectory has turning points at several values of ion-molecule separation with six reflections. This type of behavior is particularly clear in the film supplement, where this is the last collision shown. The turning points for CH_3CN can be at separations as large as 22 Å.

The rotator projection plots of figure 21 are particularly useful since they clearly demonstrate the degree of hindering. Multiple-reflection collisions are particularly easy to study for CH_3CN because the large (principal) moment of inertia assures a readily (ref. 3) interpretable trace.

Chemical Implication of Results

It has been suggested that preferential orientation of the negative end of the dipole toward the positive ion will favor a specific reaction (ref. 7). The (nearly) symmetric-top methyl alcohol (CH_3OH) is a target studied experimentally in reference 7. This polyatomic molecule has a dipole moment of 1.67 Debye units and a principal axis moment of inertia about one-half that of CH_3CN. Since the hindering is not very sensitive to the second moment of inertia (about the symmetry axis), the behavior of CH_3OH should be very similar to that of CH_3CN. The hindering will probably be less pronounced since the dipole moment is lower in CH_3OH. The fraction of collisions in which hindering occurs for CH_3OH can be calculated by a statistical study of plots of the orientation angle γ for a fixed impact parameter. The product of this fraction and the capture cross section should provide a reaction cross section which might be compared with experiment. The number of multiple reflections also increases the probability of reaction if vibrational excitation is required for reaction.

Motion-Picture Evidence for Hindered Rotation

Seven motion-picture frames from a CH_3CN single-reflection collision are shown in figure 22. In frame 1, the ion and polar molecule approach each other with the former slightly above the plane and the latter slightly below. The dipole has completed a clockwise swing. In frame 2, the particles are slightly closer, with the dipole swinging counterclockwise. The dipole continues this swing in frame 3 and completes it as reflection occurs in frame 4. The dipole completes another clockwise swing as the reflected particles retreat from each other (ion above the plane, dipole below it) in frame 5. The dipole continues a counterclockwise swing as the separation becomes large in frames 6 and 7. The translational motion of ion and molecule for frames 1 to 7 is traced with the dashed line in frame 7.

CONCLUDING REMARKS

Motion pictures made with a computer-plotter system provide new information, as well as complement time history plots of collision variables. The motion pictures allow for instantaneous correlation of translational (ion) and rotational (dipole) motion and suggest more detailed qualitative interpretation of time histories. The time histories, in turn, provide direct quantitative data on values of velocity and rotational energy and ion-molecule multiple-reflection turning points. The frequencies of rotational energy oscillations can be calculated from the plots, whereas the nature of the motion (free or hin-

dered rotation) is obtained from the motion pictures.

The usefulness of the motion-picture and time-history approach to ion-molecule studies has been established. The extension of these techniques to vibrational motion and charge exchange is straightforward. The primary limitation is in the manner in which the motion can be displayed.

Lewis Research Center,
National Aeronautics and Space Administration,
Cleveland, Ohio, March 6, 1970,
129-02.

REFERENCES

1. Dugan, John V., Jr.; and Magee, John L.: Semiclassical Approach to Capture Collisions Between Ions and Polar Molecules. NASA TN D-3229, 1966.

2. Dugan, John V., Jr.; and Magee, John L.: Capture Collisions between Ions and Polar Molecules. J. Chem. Phys., vol. 47, no. 9, Nov. 1, 1967, pp. 3103-3113.

3. Dugan, John V., Jr.; Rice, James H.; and Magee, John L.: Calculation of Capture Cross Sections for Ion - Polar-Molecule Collisions Involving Methyl Cyanide. NASA TM X-1586, 1968.

4. Dugan, J. V., Jr.; Rice, J. H.; and Magee, J. L.: On the Nature of Ion-Molecule Collisions. Chem. Phys. Letters, vol. 2, no. 4, Aug. 1968, pp. 219-222.

5. Dugan, J. V., Jr.; Rice, J. H.; and Magee, J. L.: Evidence for Long-Lived Ion-Molecule Collision Complexes from Numerical Studies. Chem. Phys. Letters, vol. 3, no. 5, May 1969, pp. 323-326.

6. Dugan, John V., Jr.; and Rice, James H.: A Computer Plotting Description of Ion-Molecule Collisions with Long-Lived Capture Complexes. NASA TN D-5407, 1969.

7. Leger, L. J.; and Meisels, G. G.: Preferred Dipole Orientation in Ion - Polar Molecule Reactions. Chem. Phys. Letters, vol. 1, no. 13, Apr. 1968, pp. 661-664.

8. Kannenberg, Robert G.: Cinematic - FORTRAN Subprograms for Automatic Computer Microfilm Plotting. NASA TM X-1866, 1969.

9. Hirschfelder, Joseph O.; Curtiss, Charles F.; and Bird, R. Byron: Molecular Theory of Gases and Liquids. John Wiley & Sons, Inc., 1964 (corrected printing) pp. 1028, 1110-1112.

TABLE I. - RESULTS FOR MULTIPLE-REFLECTION COLLISIONS

Ion-molecule pair	Impact parameter, b, Å	Location of reflecting barrier, r_c, Å	Number of cases, n	Langevin potential maximum, r*, Å	Range of numerical interaction radius, defining collision time, Å	Fraction of cases resulting in multiple reflection, f_R	Maximum number of reflections, N_{max}	Average single-reflection time, $\overline{\tau}_o$, sec	Most probable number of multiple reflections, N_M	Average collision time for multiple reflection, $\overline{\tau}_R$, sec	Maximum collision time, τ_{max}, sec
$Ar^+ + Co$	2.0	1.0	33	16.5	5 to 8	0.63	15	1.5×10^{-12}	6	6.0×10^{-12}	1.7×10^{-11}
	3.0	1.5	21	11.0	4 to 8	.13	5	2.5	2	6×10^{-12} to 7×10^{-12}	8.2×10^{-12}
	3.0	3.0	12	11.0	5 to 8	.08	3	$\sim10^{-12}$	3	1.7×10^{-11}	1.7×10^{-11}
	4.0	1.0	24	8.2	4 to 8	.33	18	1.5×10^{-12}	7	4×10^{-12}	8×10^{-12}
	6.0	1.0	49	5.5	4 to 8	.65	42	2.8	8	1.2×10^{-11}	3.5×10^{-11}
	6.0	2.0	23	5.5	5 to 8	.60	54	4	7	$\sim10^{-11}$	2.7
$NO_2^+ + HCl$	1.0	1.0	10	8.5	~10	0.30	1115	1.5×10^{-12}	20	3.3×10^{-11}	7.5×10^{-11}
	4.0	2.0	40	8.5	8 to 12	.10	40	2	4	1.5	3.1
	6.0	1.0	8	5.7	~10	.50	192	2	7	8×10^{-12} to 9×10^{-12}	2
	6.0	2.0	56	5.7	~10	.14	530	1.7	3	5×10^{-12}	6.4
	8.0	1.0	6	4.3	~10	.67	715	4	6	1.6×10^{-11}	5.2
$CH_3CN^+ + CH_3CN$	3.0	3.0	8	13.7	10	0.50	192	2×10^{-12}	7	1.7×10^{-12}	1.7×10^{-11}
	5.0	2.0	33	8.2	15 to 20	.47	[a]25	4	25	1.3×10^{-11}	2
	5.0	3.0	12	8.2	↓	.33	140	4	20	2	8
	6.0	2.0	24	6.5		.46	[a]25	5×10^{-12} to 6×10^{-12}	8	1.8	3.85
	7.0	2.0	24	5.6		.55	[a]25	4×10^{-12}	10	1.6	3.55
	8.0	2.0	12	5.2		.57	40	4.5	8	2	3.75
	10.0	2.0	12	4.1		.57	150	4.5	12	1.5	2.3
	10.0	3.0	12	4.1		.33	40	4.5	15	2	4.9

[a]Case limited to 25 reflections to minimize computer time.

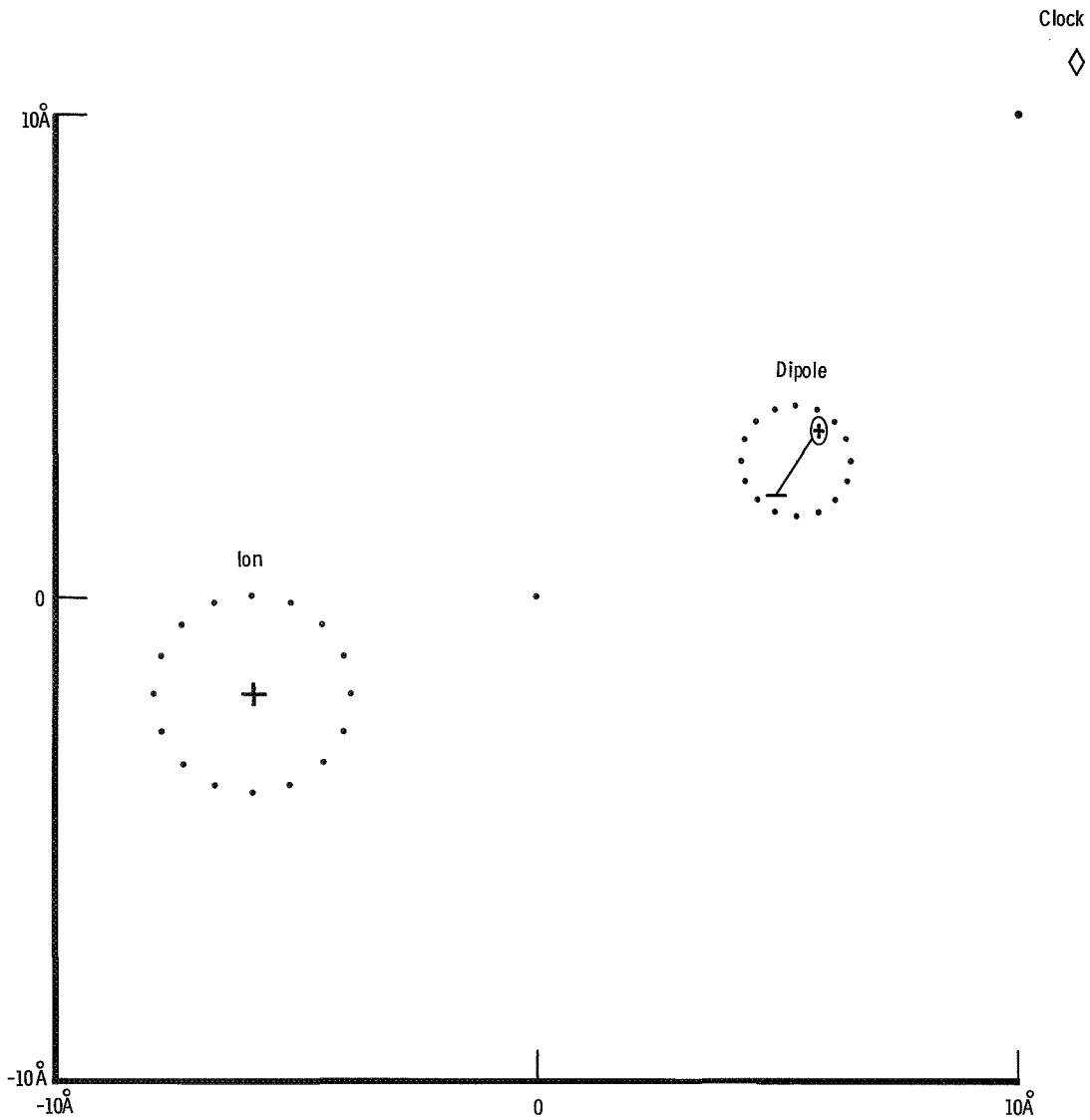

Figure 1. - Sample motion-picture frame. CS-51925

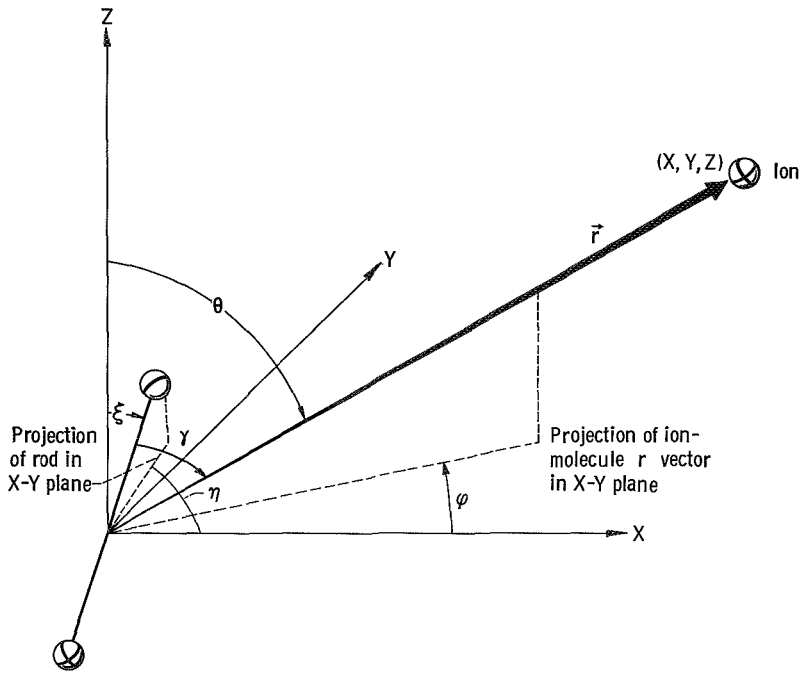

Figure 2. - Coordinate system used in computer study of interaction between an ion and a linear polar molecule.

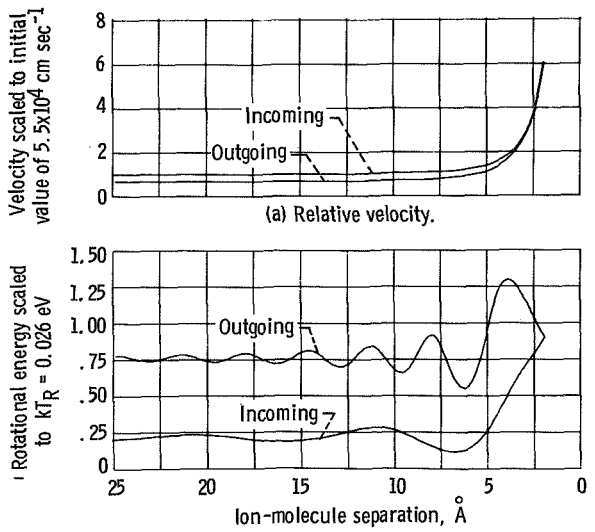

Figure 3. - Variations of ion-molecule relative velocity and polar-molecule rotational energy during $Ar^+ + CO$ single-reflection capture collision.

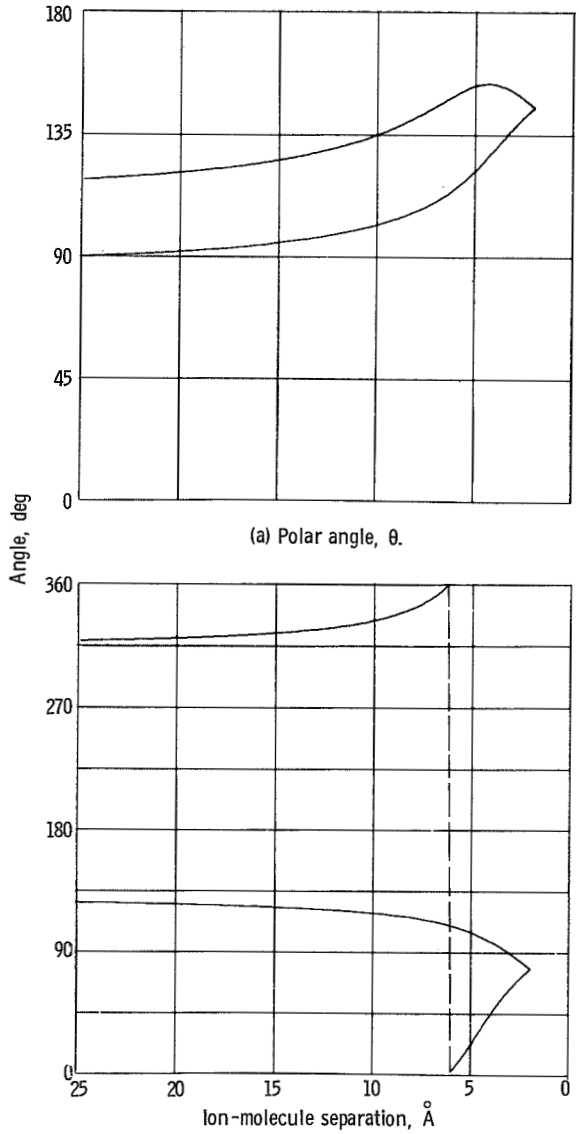

(a) Polar angle, θ.

(b) Azimuthal angle, φ; vertical dashed line indicates passing through 0 or 2π.

Figure 4. - Variations of coordinate angles for argon ion relative to CO molecule during capture collision with a single reflection.

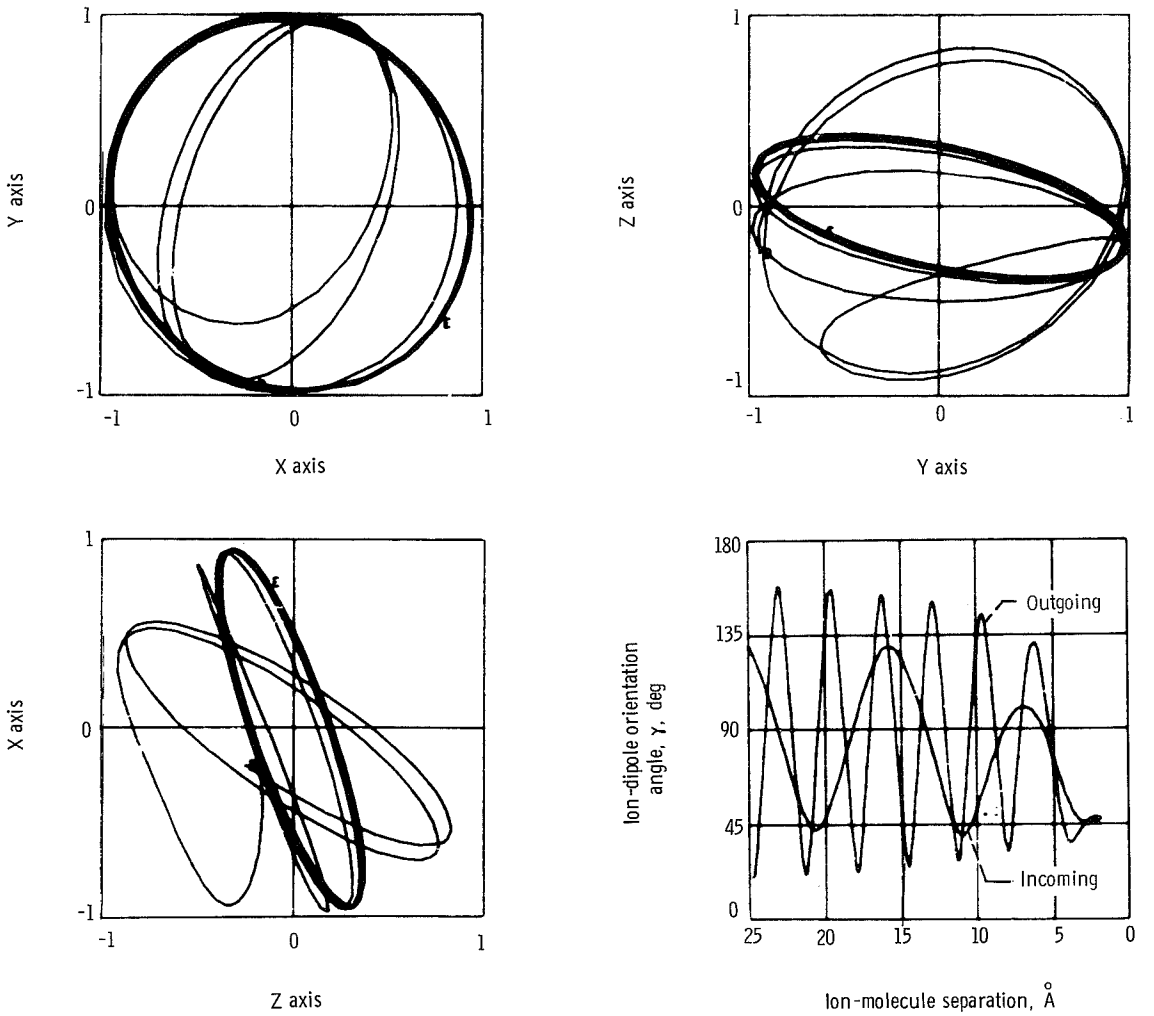

Figure 5. - Variations of dipole moment unit vector and ion-dipole orientation angle during Ar^+ + CO single-reflection capture collision.

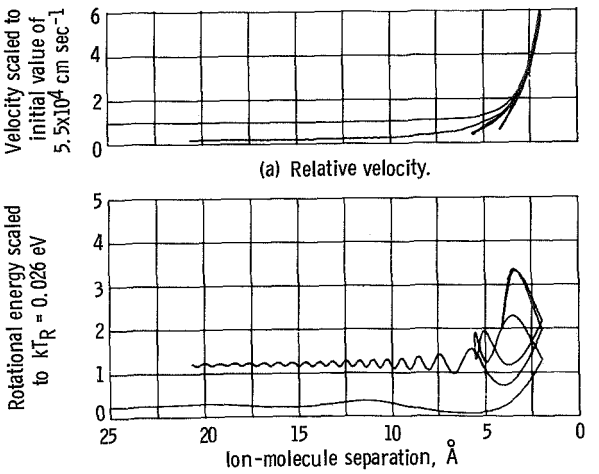

Figure 6. - Variation of ion velocity and polar-molecule rotational energy during Ar^+ + CO multiple-reflection capture collision.

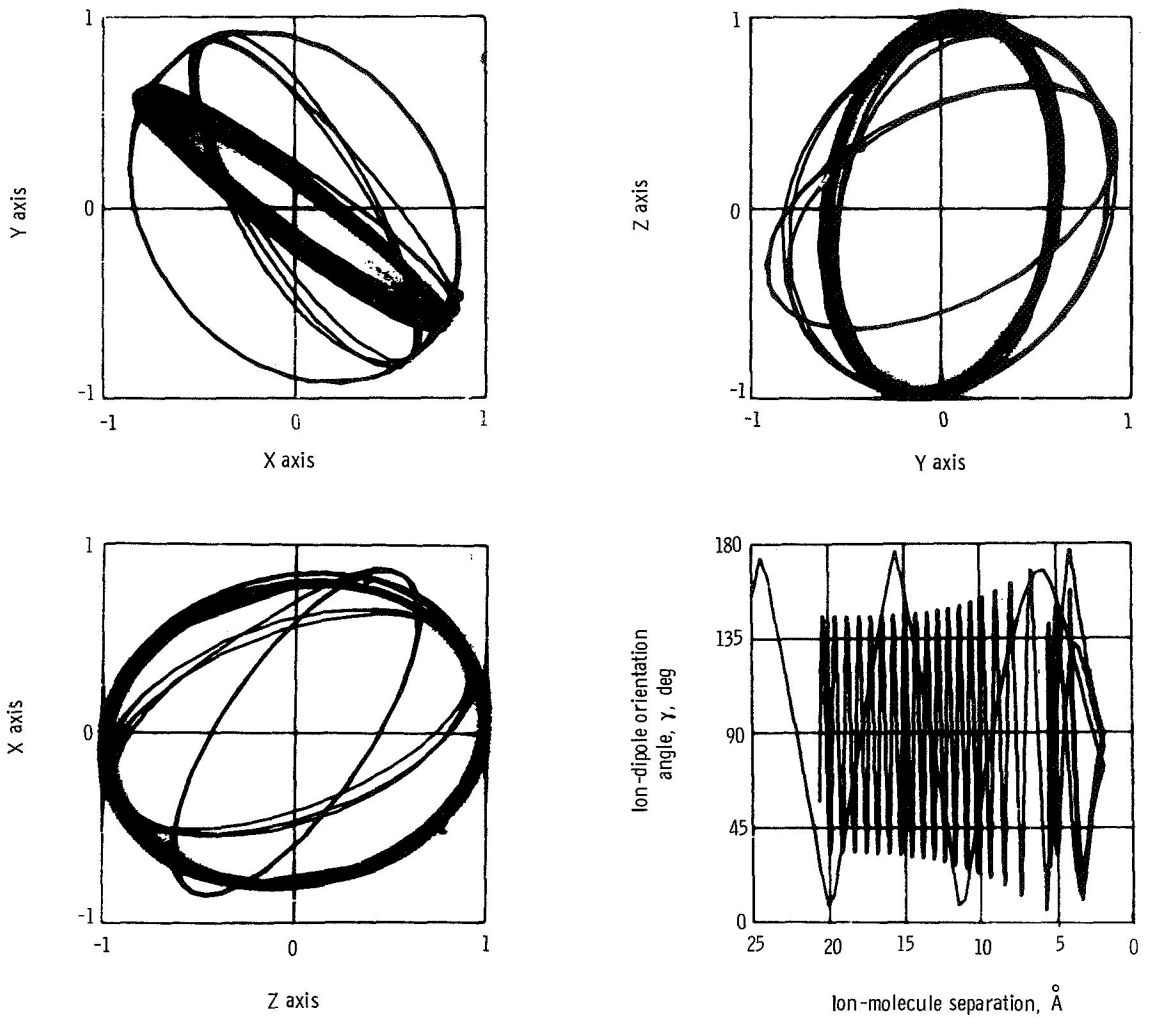

Figure 7. - Variations of dipole moment vector and ion-dipole orientation angle (between ion-molecule radius vector and negative end of dipole) during Ar^+ + CO multiple-reflection capture collision.

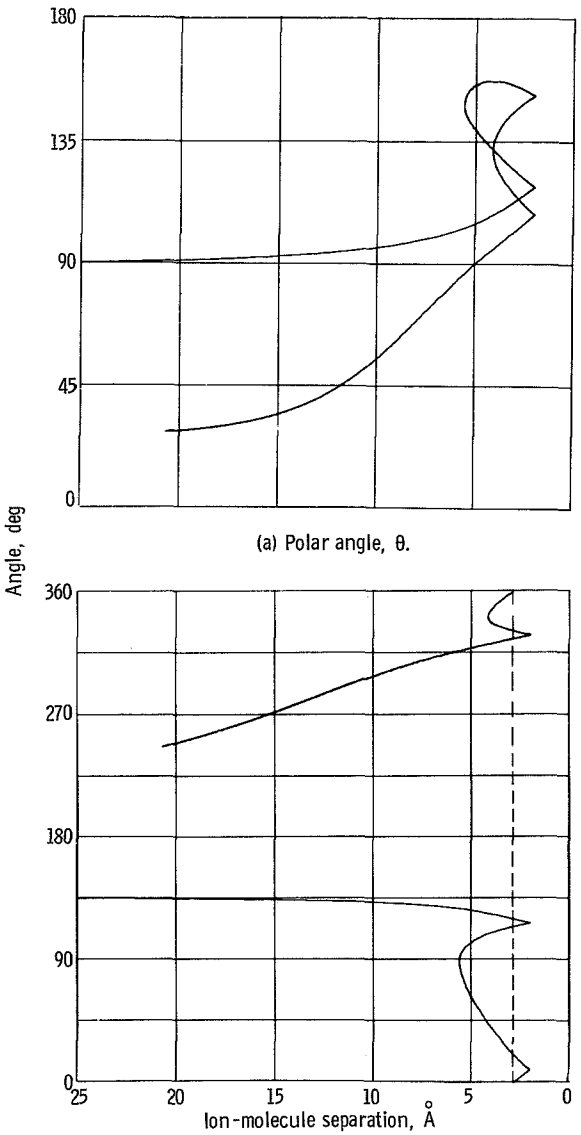

(a) Polar angle, θ.

(b) Azimuthal angle, φ; vertical dashed line indicates passing through 0 or 2π.

Figure 8. - Variations of coordinate angles for argon ion relative to CO molecule during capture collision with multiple reflections.

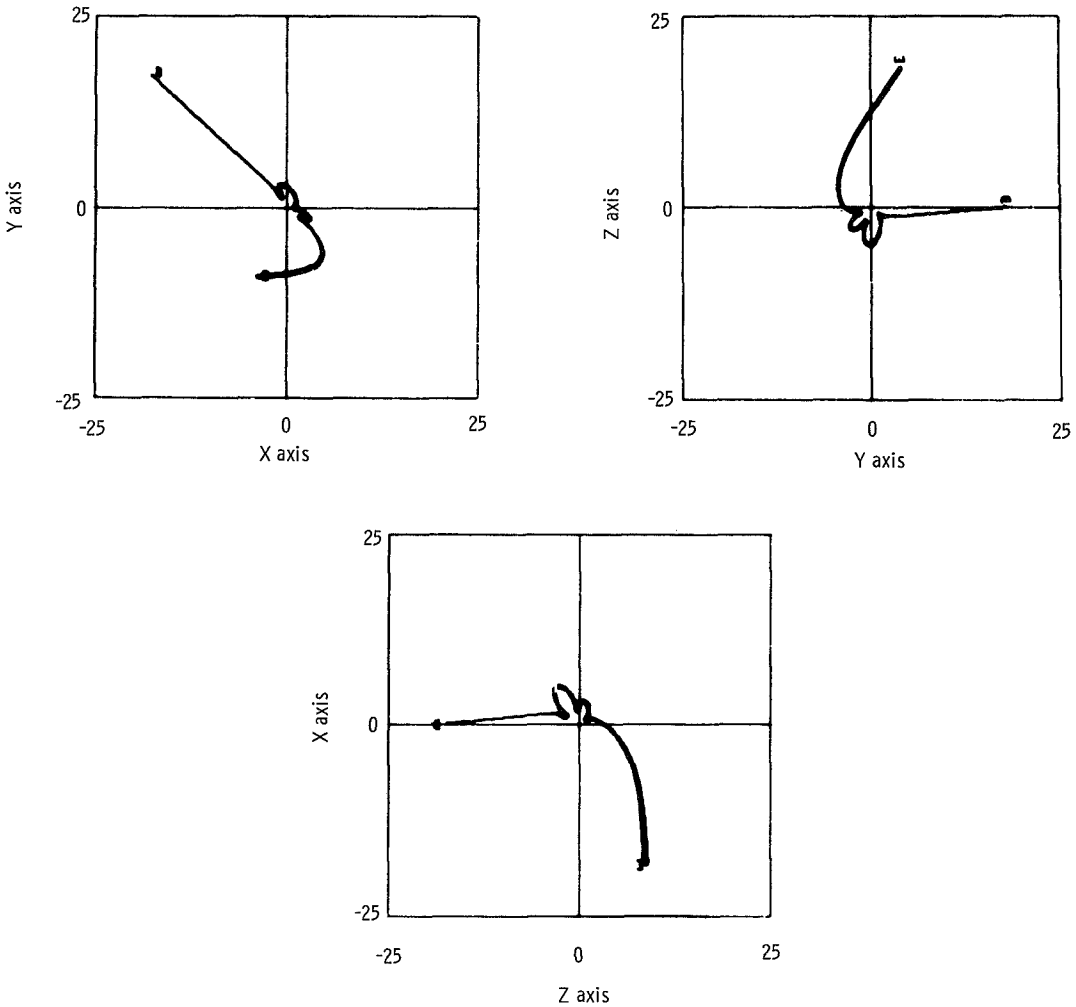

Figure 9. - Variation of ion projections tracing translational motion in $Ar^+ + CO$ capture collision with multiple reflections.

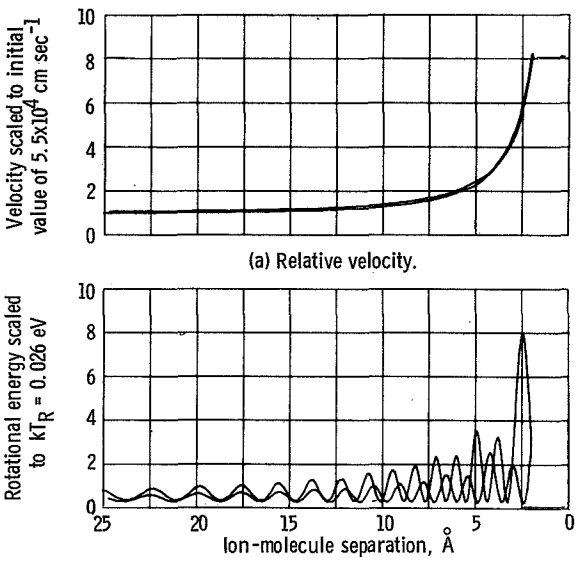

Figure 10. - Variation of ion velocity and polar-molecule rotational energy during NO_2^+ + HCl single-reflection capture collision.

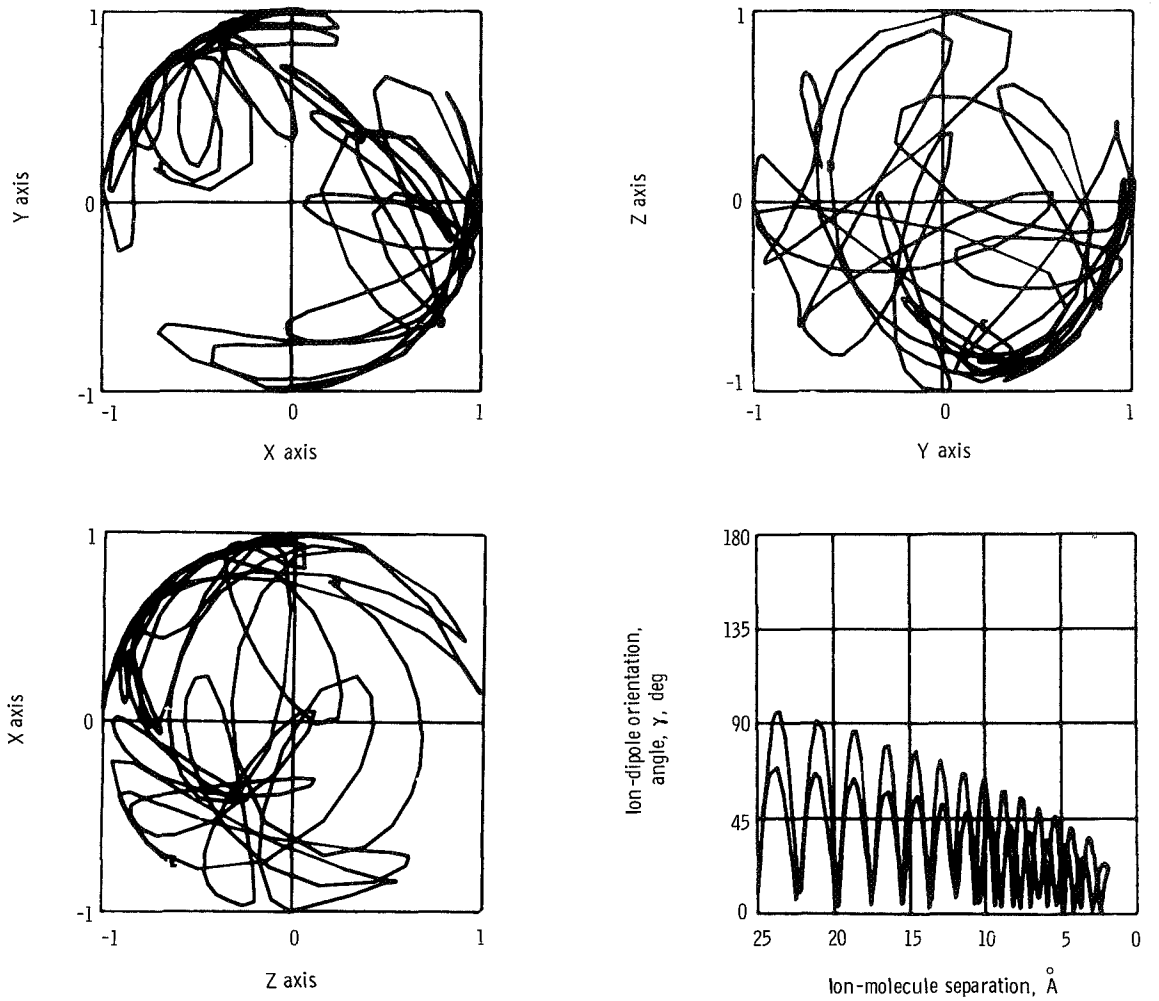

Figure 11. - Variations of dipole moment unit vector and ion-dipole orientation angle during NO_2^+ + HCl single-reflection capture collision.

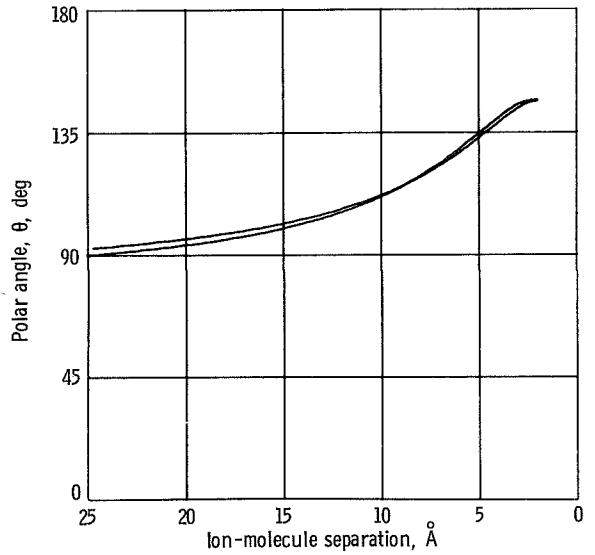

Figure 12. - Variation of polar angle for NO_2^+ ion relative to HCl molecule during single-reflection capture collision.

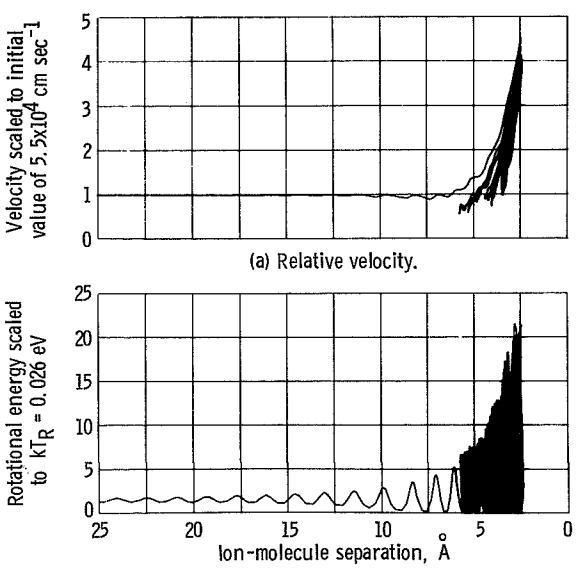

Figure 13. - Variations of ion-molecule relative velocity and polar-molecule rotational energy during NO_2^+ + HCl multiple-reflection capture collision.

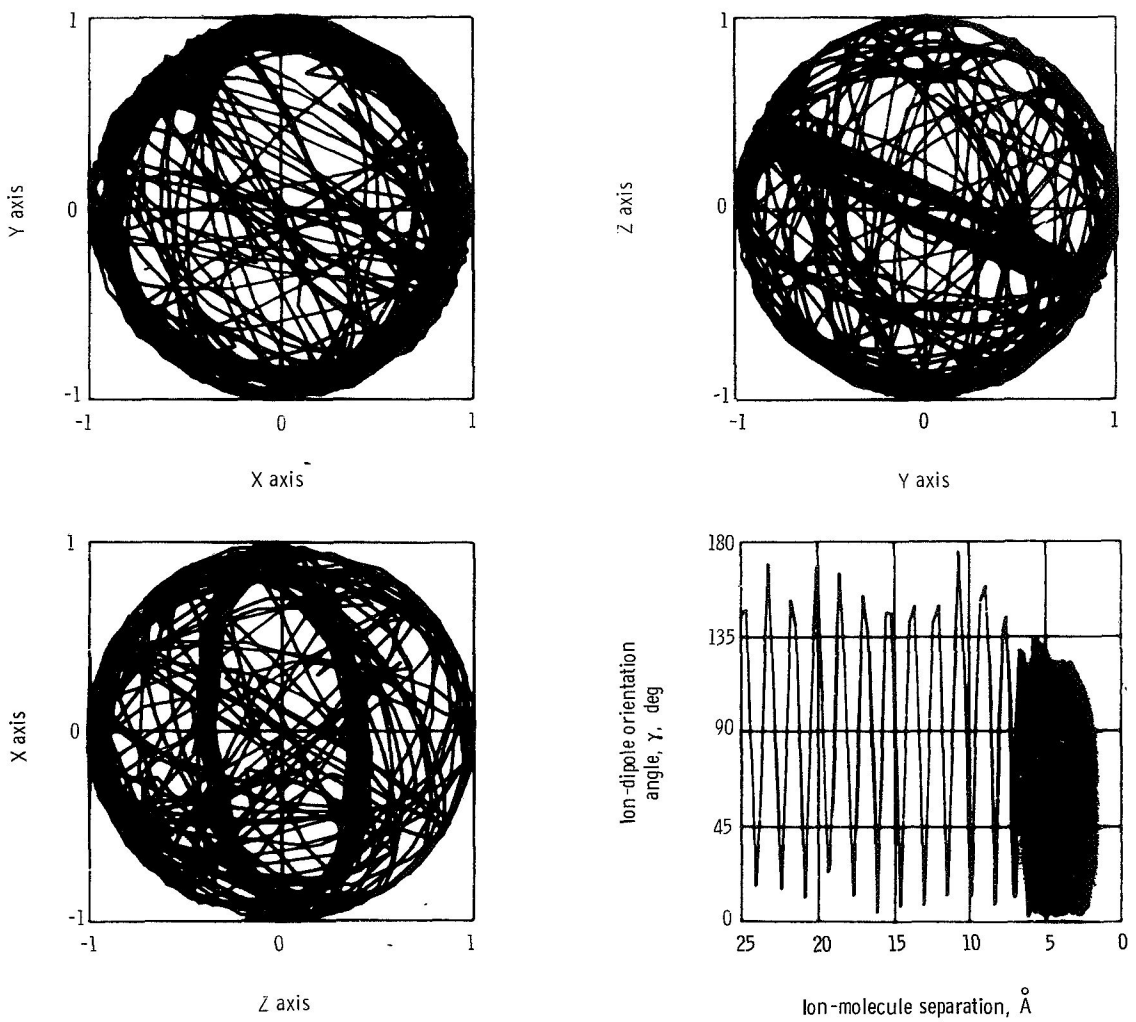

Figure 14. - Variations of dipole moment unit vector and ion-dipole orientation angle during NO_2^+ + HCl multiple-reflection capture collision.

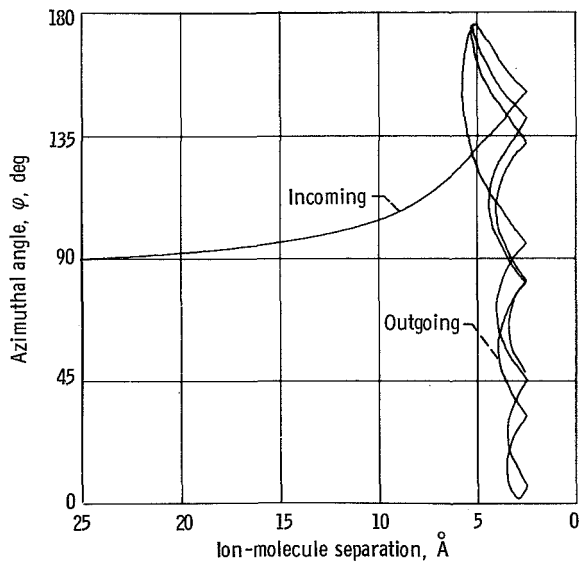

Figure 15. - Variations of azimuthal angle for translational motion of NO_2^+ relative to HCl molecule during multiple-reflection capture collision.

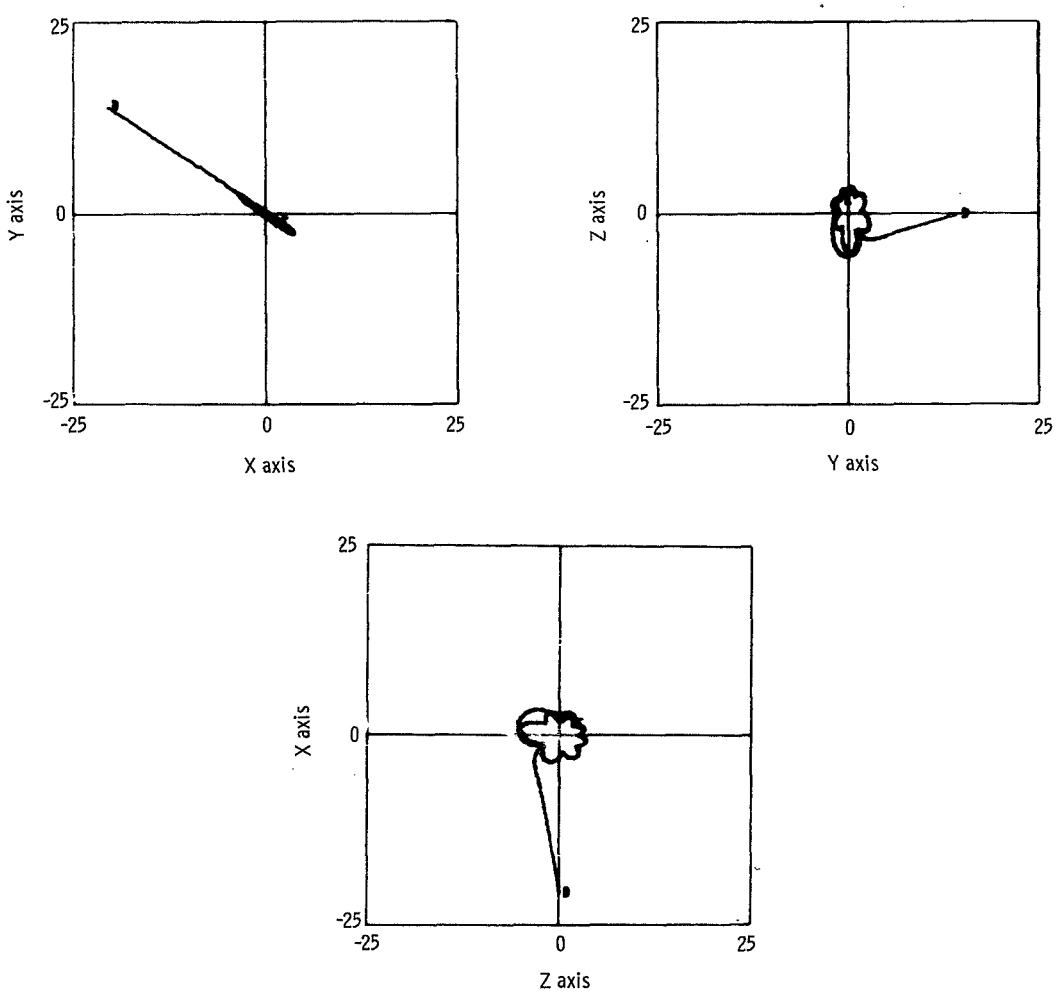

Figure 16. - Variation of ion coordinates for NO_2^+ + HCl multiple-reflection capture collision.

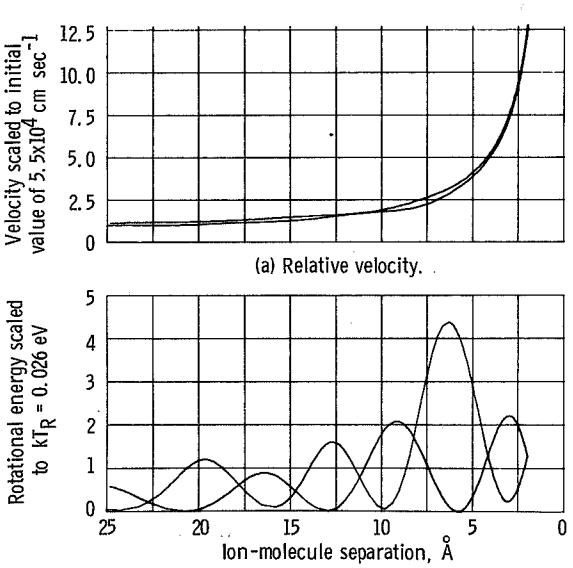

Figure 17. - Variations of ion-molecule relative velocity and polar-molecule rotational energy during CH_3CN - parent ion capture collision with a single reflection.

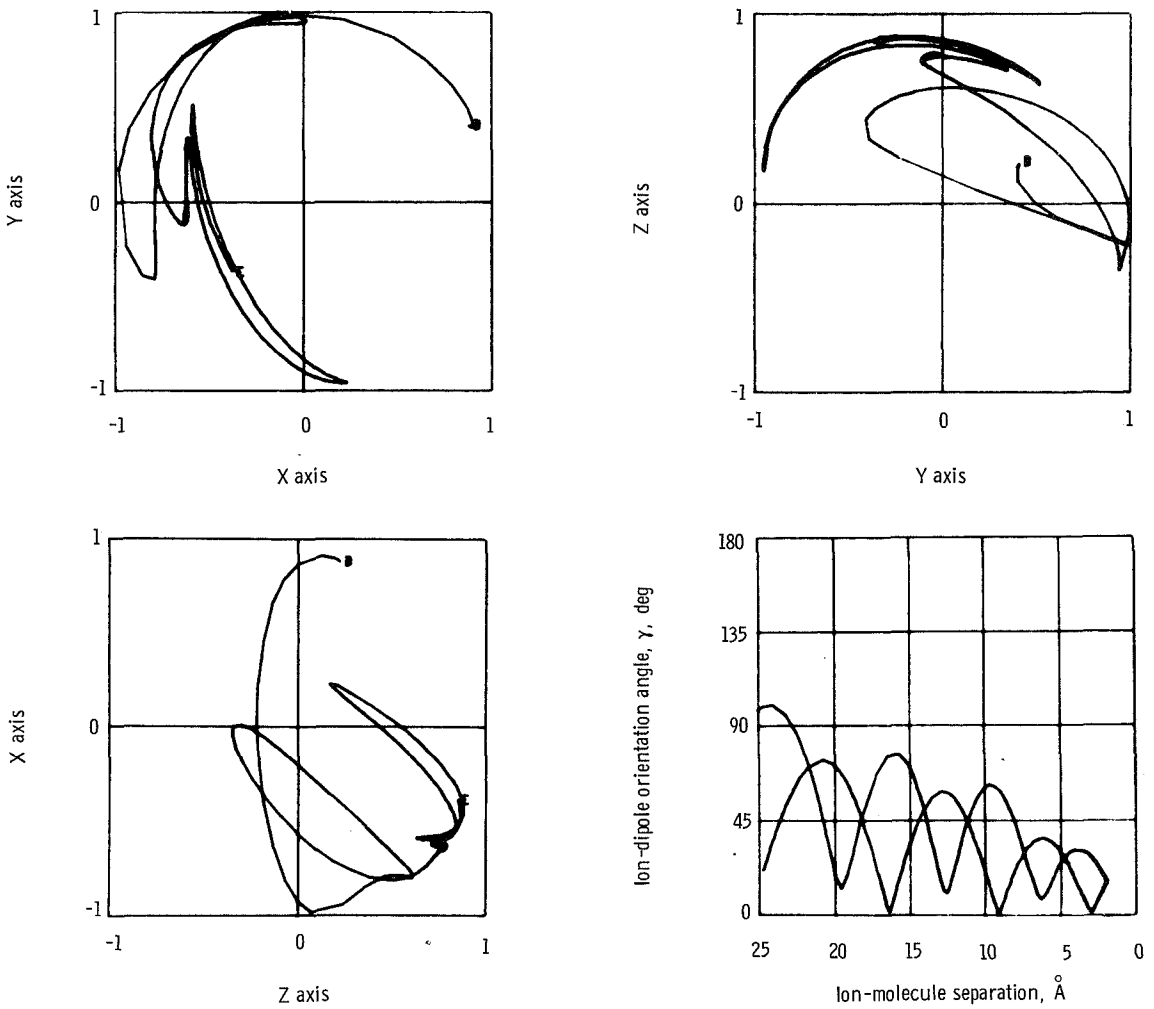

Figure 18. - Variations of dipole moment unit vector and ion-dipole orientation angle during CH_3CN - parent ion capture collision with a single reflection.

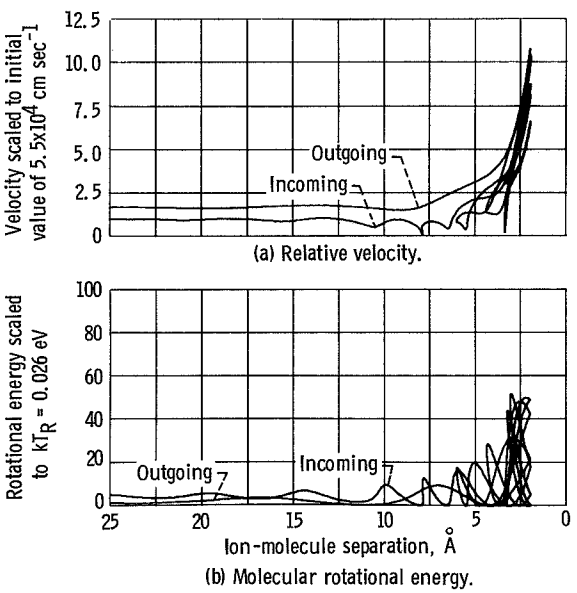

Figure 19. - Variation of ion velocity and polar-molecule rotational energy during CH_3CN - parent ion multiple-reflection capture collision.

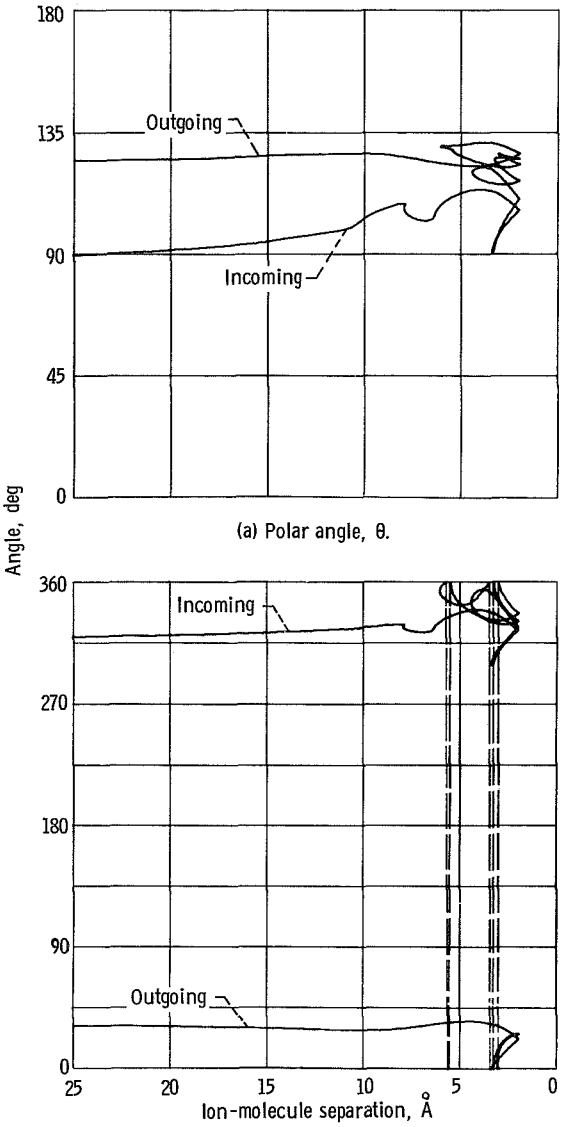

(a) Polar angle, θ.

(b) Azimuthal angle, φ; vertical dashed lines indicate passing through 0 or 2π.

Figure 20. - Variations of coordinate angle for CH_3CN^+ relative to CH_3CN molecule during capture collision with multiple reflections.

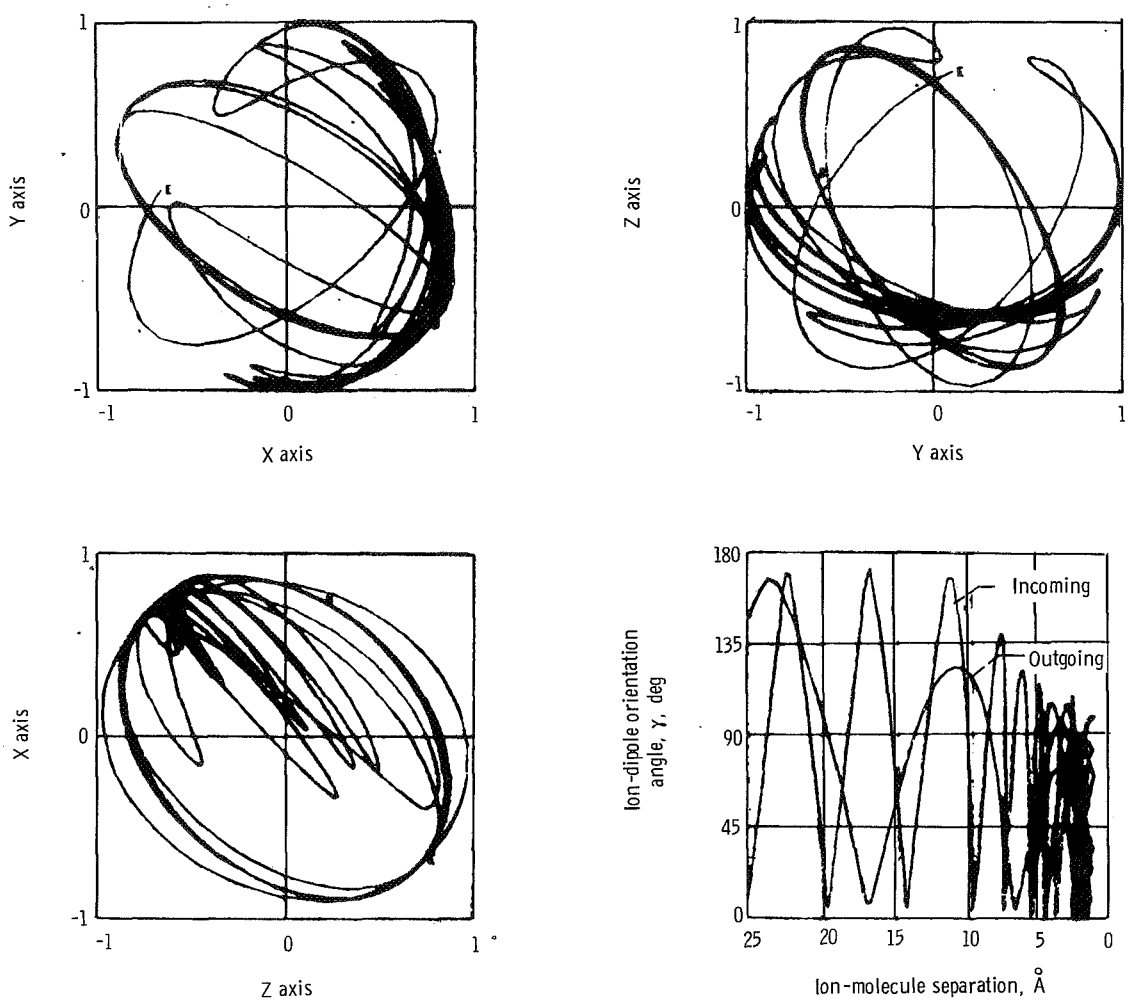

Figure 21. - Variations of dipole moment vector and ion-dipole orientation angle during CH_3CN - parent ion multiple-reflection capture collision with several turning points.

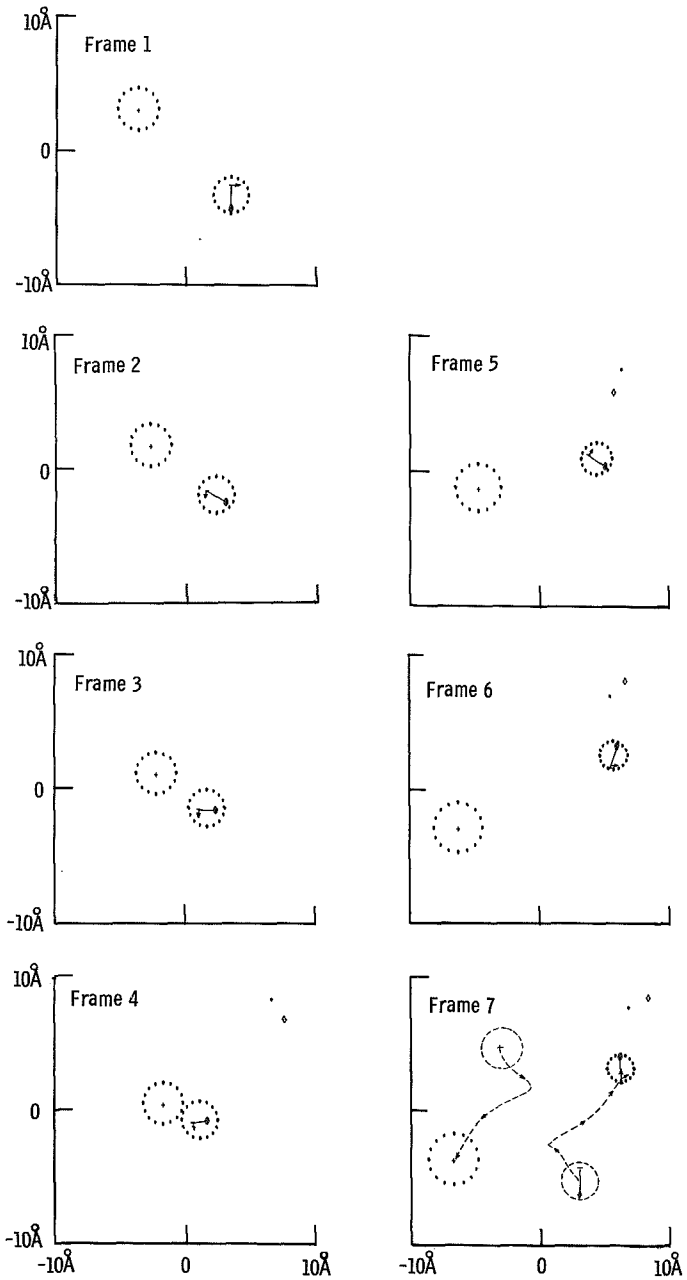

Figure 22. - Motion-picture evidence for hindered rotation in frames 1 to 7 for $CH_3CN^+ + CH_3CN$ single-reflection collision.

Motion-picture film supplement C-269 is available on loan. Requests will be filled in the order received.

The film (16 mm, 12 min, color, sound) consists of 11 separate collision sequences involving the polar target molecules CO, HCl, and CH_3CN. The collisions are single- and multiple-reflection types demonstrating mutual spiraling of the collision partners as well as hindering of the dipole by the incident ion.

Film supplement C-269 is available on request to:

Chief, Management Services Division (5-5)
National Aeronautics and Space Administration
Lewis Research Center
21000 Brookpark Road
Cleveland, Ohio 44135

CUT

Date _____

Please send, on loan, copy of film supplement C-269 to
TN D- 5747

_____

Name of Organization

_____

Street Number

_____

City and State Zip Code

Attention: Mr. _____

Title _____

Place
stamp
here

Chief, Management Services Division (5-5)
National Aeronautics and Space Administration
Lewis Research Center
21000 Brookpark Road
Cleveland, Ohio 44135

NATIONAL AERONAUTICS AND SPACE ADMINISTRATION
WASHINGTON, D. C. 20546
OFFICIAL BUSINESS

FIRST CLASS MAIL

POSTAGE AND FEES PAID
NATIONAL AERONAUTICS ANI
SPACE ADMINISTRATION

POSTMASTER: If Undeliverable (Section 158 Postal Manual) Do Not Return

"The aeronautical and space activities of the United States shall be conducted so as to contribute . . . to the expansion of human knowledge of phenomena in the atmosphere and space. The Administration shall provide for the widest practicable and appropriate dissemination of information concerning its activities and the results thereof."

—NATIONAL AERONAUTICS AND SPACE ACT OF 1958

NASA SCIENTIFIC AND TECHNICAL PUBLICATIONS

TECHNICAL REPORTS: Scientific and technical information considered important, complete, and a lasting contribution to existing knowledge.

TECHNICAL NOTES: Information less broad in scope but nevertheless of importance as a contribution to existing knowledge.

TECHNICAL MEMORANDUMS: Information receiving limited distribution because of preliminary data, security classification, or other reasons.

CONTRACTOR REPORTS: Scientific and technical information generated under a NASA contract or grant and considered an important contribution to existing knowledge.

TECHNICAL TRANSLATIONS: Information published in a foreign language considered to merit NASA distribution in English.

SPECIAL PUBLICATIONS: Information derived from or of value to NASA activities. Publications include conference proceedings, monographs, data compilations, handbooks, sourcebooks, and special bibliographies.

TECHNOLOGY UTILIZATION PUBLICATIONS: Information on technology used by NASA that may be of particular interest in commercial and other non-aerospace applications. Publications include Tech Briefs, Technology Utilization Reports and Notes, and Technology Surveys.

Details on the availability of these publications may be obtained from:

SCIENTIFIC AND TECHNICAL INFORMATION DIVISION

NATIONAL AERONAUTICS AND SPACE ADMINISTRATION

Washington, D.C. 20546